Deep Neural Network-based Reversible Image Steganography Technique using Circle-U-Net

N. Malarvizhi[1,*], R. Priya[1], R. Bhavani[1]
[1]Department of Computer Science and Engineering, Annamalai University, Chidambaram, India
Emails: nmalarvizhi16@gmail.com; prykndn@yahoo.com; bhavaniaucse@gmail.com

Abstract

Data communication is made at the ease with the advent of the latest communications medium and tools. The concern over data breaches has increased. The digital media communicated across the network are susceptible to unapproved access. Though numerous image steganography approaches were existing for concealing the secret image into the cover image there are still limitations such as inadequate restoration of image quality and less embedding capacity. To overwhelm such shortcomings recently many image steganography approaches based on deep learning are proposed. In this work, a Circle-U-Net-based reversible image steganography technique is proposed. The model includes a contracting process, which includes residual bottleneck as well as circle connect layers which obtain context; an expanding process, which includes sampling layers as well as merging layers for pixel-wise localization. The reversible image steganography (RIS) is carried out with neural network models such as CNN, U-Net scheme, and Circle-U-Net structure on TinyImageNet-200 and Alzheimer's MRI dataset. The proposed technique is experimented along with RIS using CNN and RIS using U-Net. The experimental results depict that the RIS using the Circle-U-Net structure performs better among the three models.

Keywords: Reversible Image Steganography; Convolutional Neural Network; Circle-U-Net; Deep Learning

1. Introduction

The advancement of communication technologies leads to the communication of a significant quantity of images through the internet. These images are saved in the cloud storage. However, these images require proper access authorization to avoid access from unauthorized users. Safeguarding the confidentiality of communication between two individuals/groups/organizations has become a major area of research for over two decades. The potential approach to deal with this topic is the activity of hiding the secret image (S_I) in the cover image (C_I). This approach doesn't affect the visible feature of an image. Though authorized users can obtain the S_I from C_I. This approach is known as image steganography (IS) which is an essential procedure of information hiding. It has a huge necessity in the field of digital communication and has a broad variety of applications such as healthcare, e-commerce, military communication, copyright protection, and many others.

The approaches of IS can be classified as reversible and irreversible. The list of irreversible approaches is a least-significant bit (LSB) [1], pixel-value differencing (PVD) [2], subsequently proposed exchange and combination methods of PVD and LSB [3], modulus function, and histogram shifting method [4]. The major reversible approaches are proposed by Barton [5], Tian [6], Alattar [7], Kim et al. [8], Lu et al. [9], Jung [10], Carpentieri et al. [11], and Nguyen et al. [12].

In today's scenario, IS approaches built on a convolutional neural network (CNN) have received extensive research interest owing to their exceptional abilities in contrast to the traditional approaches. The performance of IS is improved in all the major aspects. The initial end-to-end encoding and decoding architecture established on CNN is given in [13]. An autoencoder and decoder structure is given in [14]. In this structure, the three different networks such as preparation, hiding, and reveal networks are prepared. The first one converts the Red (R), Green (G), and Blue (B) pixels of S_I into features. The second one obscures the gained features into C_I. The third one isolates S_I from C_I. This structure has increased payload capacity and quality of S_I while a comprise has been done in the restored image. A new IS scheme is offered in [15] embeds two S_I in one C_I which has a better and enhanced payload. A novel invisible IS is proposed in [16] and it is observed that it has provided enhancement of stego-image (S_G) quality. The C_I is converted to YCrCb format. The S_I is in grayscale format

Doi: https://doi.org/10.54216/FPA.130210
Received: April 17, 2023 Revised: July 19, 2023 Accepted: October 02, 2023

and to hide it the channel 'Y' is used. The other channels 'Cr' and 'Cb' is not affected, and it comprises of color information. Thus S_G quality is increased. Later CNN-based steganography is offered in [17] which improved the payload and quality of S_G.

The key contribution of the research work is

1. A CNN-based architecture has been experimented for RIS.
2. A U-Net-based architecture has been experimented for RIS.
3. A Deep Neural Network (DNN) Model based on Circle-U-Net is proposed to improve the RIS with image over an image and to provide better reconstruction.

2. Related Works

Hayes, Jamie, and George Danezis [18] applied the discriminative procedure of acquiring the knowledge of a steganographic algorithm based on adversarial training methods. By using an unsupervised learning approach, a steganographic method is created that can contend against the most advanced steganographic methods, demonstrating the efficacy of adversarial training. Baluja, Shumeet [19] tried to fit a full-color image inside another image of similar size in his research. In his research, deep neural networks are concurrently trained to generate the concealing and extracting procedures that act as a pair. His technique compresses and disseminates the representation of S_I throughout all of the usable bits, in contrast to many common $\mathbb{IS}$ techniques that encrypt the secret message inside the LSB of a C_I.

Van, T. P. et al., [20] focused on concealing S_I within C_I of identical size. To boost up the learning process, a new learning approach is suggested that employs deep CNN (Hiding Network) that shares the same architecture as U-Net. Comprehensive experiments prove that perhaps the new network architecture and training approach can contribute to a 50% reduction in training time and a 30% reduction in mean square error of pixel variation. Liu, L. et al., [21] recommended a DNN-based information hiding scheme with additional capacity, which can transform a huge color image into a much smaller one. DNN was employed for both the concealment and retrieval phases of this scheme. Additionally, the two networks have been acquired via adversarial training and then utilized in pairs. There was no significant difference between the S_I and the C_I. The suggested scheme outperformed the state-of-the-art DNN-based data-hiding schemes.

At first Deep learning (DL) was applied in the $\mathbb{IS}$ in the approach presented in [19]. In this approach, the color images are embedded in a grayscale image. The process of concealment and splitting is done by training the CNN. The deformation difficulty of color images was resolved in [22] with a further complicated and depth architecture. Later to advance the $\mathbb{IS}$ deformation performance and estimation precision a long short-term memory (LSTM) based reversible $\mathbb{IS}$ model is proposed in [23]. An alternative framework was proposed in [24] by examining reinforcement learning. It resulted in effective security performance and stable learning.

3. Proposed Work

The reversible image steganography is carried out with the neural network models such as CNN, U-Net, and Circle-U-Net structure on TinyImageNet-200 and Alzheimer's MRI dataset. The general workflow is shown in figure 1.

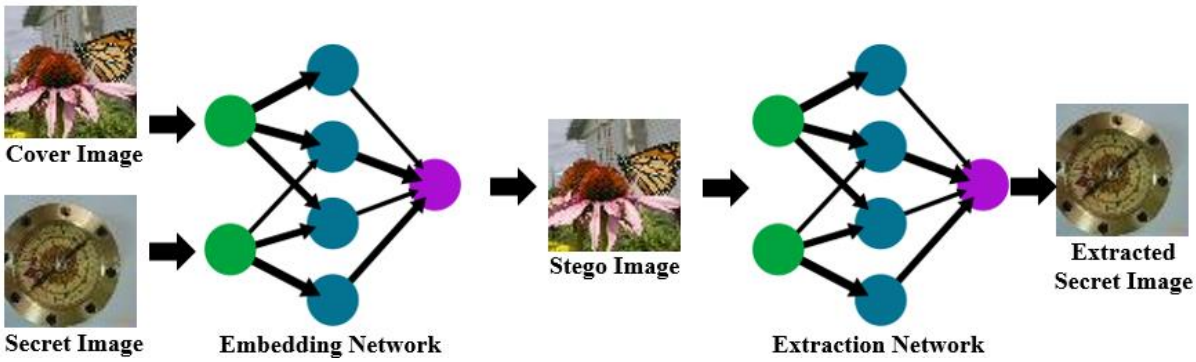

Figure 1: General Workflow of RIS

Doi: https://doi.org/10.54216/FPA.130210
Received: April 17, 2023 Revised: July 19, 2023 Accepted: October 02, 2023

3.1 RIS using CNN

RIS using CNN [25] has two architectures namely encoder and decoder. The encoder architecture is utilized to conceal the S_I in the C_I whereas the decoder architecture is used to recreate the S_I and C_I.

3.1.1 Encoder Architecture

The architecture conceals the S_I into the C_I. The size of both images is considered to be the same or the S_I should be of less size than the C_I. The architecture then utilizes a series of 3×3 convolutions along with the ReLU layers for decomposing the S_I into features. The architecture has 9 layers. Every layer consists of three Conv2D layers followed by ReLU. The last layer compresses the convoluted feature and then the Batch normalization operation is carried out to create the S_G. Batch normalization is used to speed up the training process.

3.1.2 Decoder Architecture

The architecture takes the S_G and extracts the S_I. The S_G from the encoder, architecture is considered as input and goes into a series of convolutions along with the ReLU layers to extract S_I. The architecture has 5 layers. To each layer, a 3×3 convolution is applied along with Batch normalization operation and ReLU as an activation function (A_F). In the final output layer sigmoid is used as an A_F and a S_I is extracted.

3.2 RIS using U-Net

RIS using U-Net has two networks namely the encoding network (E_N) and the decoding network (D_N) [26]. The approach constricts and disseminates S_I on each available bit on the C_I . Figure 2 shows the architecture of the RIS using U-Net. The model is evaluated in this work for the above-mentioned datasets.

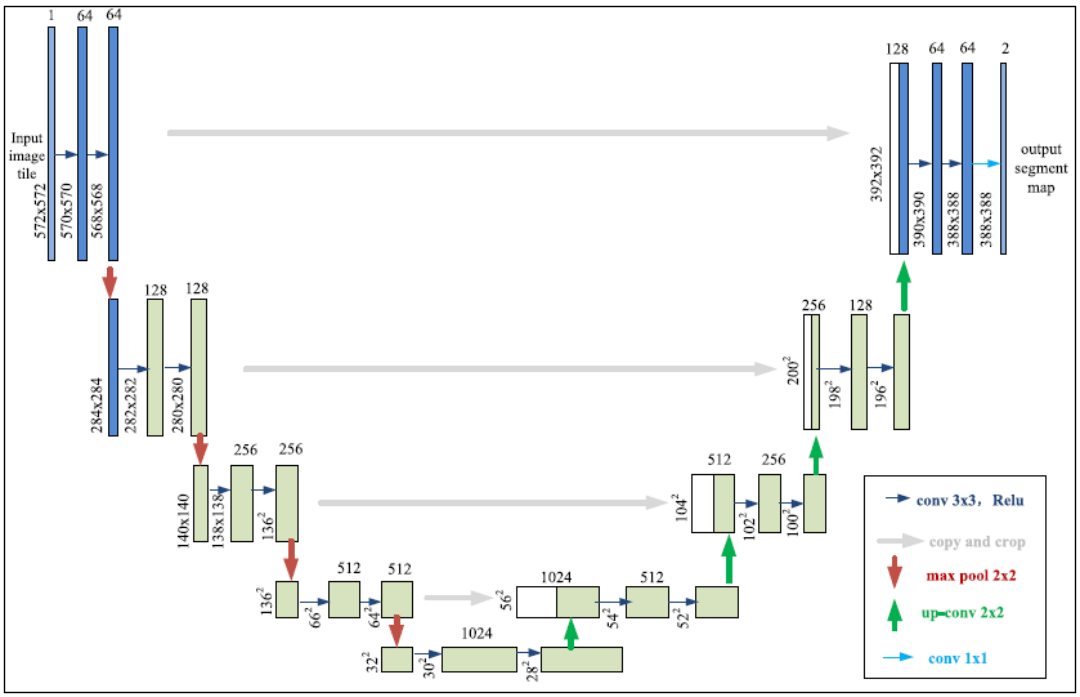

Figure 2: U-Net Architecture

3.2.1 Encoding Network

The E_N has two phases such as the contraction phase (C_P) and the expansion phase (E_P). In the C_P, the model comprises of 256×256 inputs with a 6-channel feature tensor and it is finished by a 4×4 convolution layer (C_L) in every downsampling process. Every convolution is followed by an A_F (ie., LeakyReLU) and then by Batch Normalization (B_N) operation. During downsampling, once convolution completes the feature channels are doubled. Subsequently when seven downsampling operations completes the number of feature channels becomes 512 and the feature map's (F_M) size becomes 2×2. In the E_P, upsampling of the F_M is done via a deconvolution layer of 4×4 and semi number of feature channels. Then the upsampling operation is descended through the F_M as of the C_P and the network acquires the information of F_M with various stages. In every upsampling process, a 4×4 convolutional layer is utilized each C_L is followed by an A_F and B_N. At the

Doi: https://doi.org/10.54216/FPA.130210
Received: April 17, 2023 Revised: July 19, 2023 Accepted: October 02, 2023

concluding level of the network, the feature vectors (64) are compacted into a 3 – channels F_M by utilizing 4×4 convolution and A_F to figure out the S_G.

3.2.2 Decoding Network

The D_N functionality is to recover the S_I from S_G. A plain network with 6 C_L is designed with a filter size of 3×3. The layer is followed by the ReLU and B_N operation. The B_N operation doesn't have a pooling layer and dropout operation. At the last level of the network, two outputs such as S_I and C_I are computed by mapping the 64-component feature vector to the required number of classifications using sigmoid and 3×3 convolution.

3.3 RIS using Circle-U-Net

An effective structure for the semantic segmentation of objects is named as Circle-U-Net which is a recent category of U-Net [27]. It has 101 layers which are motivated by the residual net and circle concepts from geometry. As the layers are deep and residual, the objects are segmented better than in other networks. The network has 10 ten blocks, and it begins with a 7×7 block followed by a pooling layer ($\mathcal{P}$) as $\mathcal{P}_1 \rightarrow \mathcal{P}_2$ with 3 bottleneck blocks, $\mathcal{P}_3$ with 4 bottleneck blocks with 1 circle connect, $\mathcal{P}_4$ with 23 bottleneck blocks with 2 circle connects, $\mathcal{P}_5$ with 3 bottleneck blocks with 1 circle connect. The contracting layers (ie., $\mathcal{P}_1$ to $\mathcal{P}_5$ obtains the context of the image. The expanding layers (ie., $\mathcal{P}_6$ to $\mathcal{P}_{10}$) accomplishes pixel-wise localization and forms a segmented image. $\mathcal{P}_6$ is the uniting layer from $\mathcal{P}_4$, $\mathcal{P}_7$ is the uniting layer from $\mathcal{P}_3$, $\mathcal{P}_8$ is the uniting layer from $\mathcal{P}_2$, $\mathcal{P}_9$ is the uniting layer from $\mathcal{P}_1$, and $\mathcal{P}_{10}$ is the ending expanding layer and generates the output via pixel-wise classification. Its architecture is shown in figure 3.

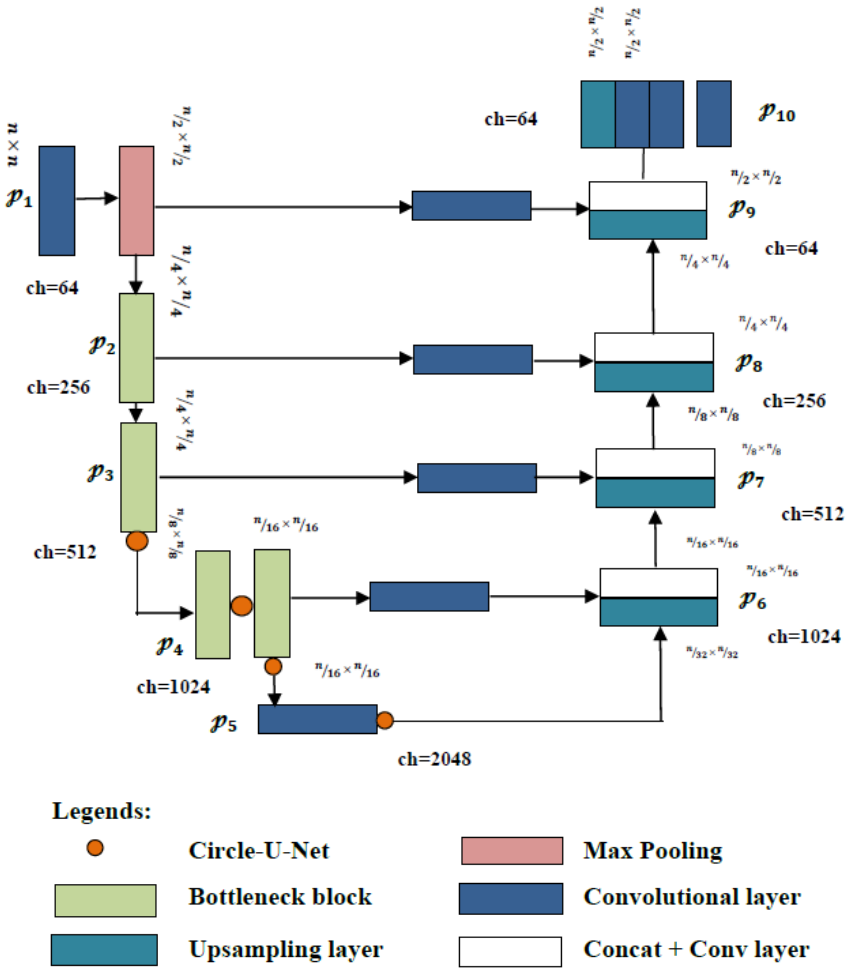

Figure 3: Circle-U-Net Architecture

Doi: https://doi.org/10.54216/FPA.130210
Received: April 17, 2023 Revised: July 19, 2023 Accepted: October 02, 2023

3.3.1 Hiding Network

The precise performance of the model parameter selections is analogous to the formation of the Circle-U-Net system, as shown in Figure 3, as well as the concealed network discussed in this portion includes both a contraction process and also an expansion process. All deep neural networks comprise a contraction stage. In contrast to the Circle-U-Net network, this one has a pooling layer, three bottleneck layers in $\mathcal{P}_2$, and four bottleneck layers in $\mathcal{P}_3$. The source is a 256X256 descending 64-channel feature tensor. and then a C_L for every phase of the downsampling process. Following every convolution is a LeakyReLU A_F as well as a B_N operation. This is done so that network training can be completed more quickly. After each iteration of the downsampling process that involves convolution, we increase the number of feature channels by dual. There is a circle link that extends from $\mathcal{P}_2$ to $\mathcal{P}_5$, and it helps improve the structure that conceals the image. Following seven iterations of downsampling, the total number of feature channels has been decreased to 512, and the dimension of the F_M is 2 X 2. A deconvolution layer (DeConv) with dimensions of 4X4 is used to upsample the F_M during the expansion phase, significantly reducing the number of feature channels in the process. At such a point, the F_M learned in the contraction phase is concatenated with the F_M learned in the expansion phase, having allowed the network to acquire F_M by both phases.

3.3.2 Extraction Network

We constructed a CNN to obtain concealed images from S_G made by hiding networks, also referred to as recovery networks. We examined the recovery network's layout to accurately recover data from concealed networks. The created network is a "simple network" of six C_L, through contrast towards the concealed network structure. To enhance the neural network's non-linear learning ability, CNN makes employs the dropout process, A_F, and pooling layer. The aim of a CNN is to understand the appropriate parameters automatically utilizing nonlinear features. The weight parameters of every level of the CNN are adapted during training to enhance the input-to-output mapping. CNN has an effect similar to linear multivariate equations whenever the effects of these nonlinear processes are considered. With this in consciousness, we thought up a structure wherein the filter size of every convolutional layer is 3X3, with both a ReLU activation and B_N operation following every convolutional layer even without a pooling layer or dropout functionality. The final layer of this network utilizes a 3X3 convolution and the Sigmoid as A_F to generate the two outcomes, the hidden picture, and the C_I, from the 64-component feature vectors

4. Experimental Analysis

4.1 Experimental Setup

The experiment is carried out with GPU T4 x 2 with 16GB of RAM. Python 3.10 is used as a programming language. TinyImageNet-200 [28] (which contains 1,00,000 images) and the Alzheimer MRI dataset [29] (which contains 6400) are used for experimental evaluation.

4.2 Performance Metrics

PSNR and SSIM are taken as the performance metrics to assess the proposed work.

PSNR: Peak Signal-to-Noise Ratio is utilized to distinguish the resemblance between the recovered and the original image.

$$\text{PSNR} = 20\log_{10}\left(\frac{255}{\text{RMSE}}\right)$$

SSIM: Structural Similarity Index Measure is utilized for the calculation of image quality based on an original uncompressed or distortion-free image as a source.

4.3 Experimental Results and Discussion

The sample images for cover and secret images of TinyImageNet-200 dataset are shown in figure 4 and figure 5. The sample images for cover and secret images of Alzheimer MRI dataset are shown in figure 6 and figure 7.

Doi: https://doi.org/10.54216/FPA.130210
Received: April 17, 2023 Revised: July 19, 2023 Accepted: October 02, 2023

(a) img1

(b) img2

(c) img3

(d) img4

(e) img5

(f) img6

Figure 4: Sample Cover Images of TinyImageNet-200 dataset

(a) img1

(b) img2

(c) img3

(d) img4

(e) img5

(f) img6

Figure 5: Sample Secret Images of TinyImageNet-200 dataset

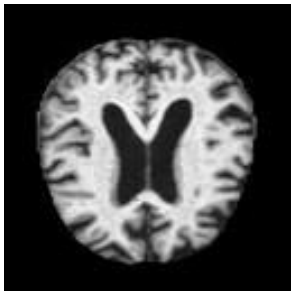

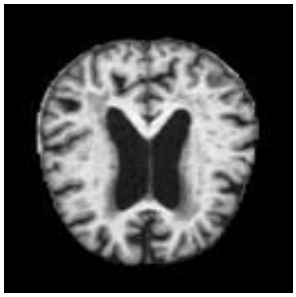

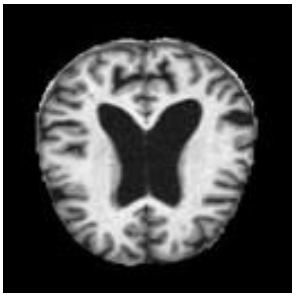

Doi: https://doi.org/10.54216/FPA.130210
Received: April 17, 2023 Revised: July 19, 2023 Accepted: October 02, 2023

(a) img1 (b) img2 (c) img3

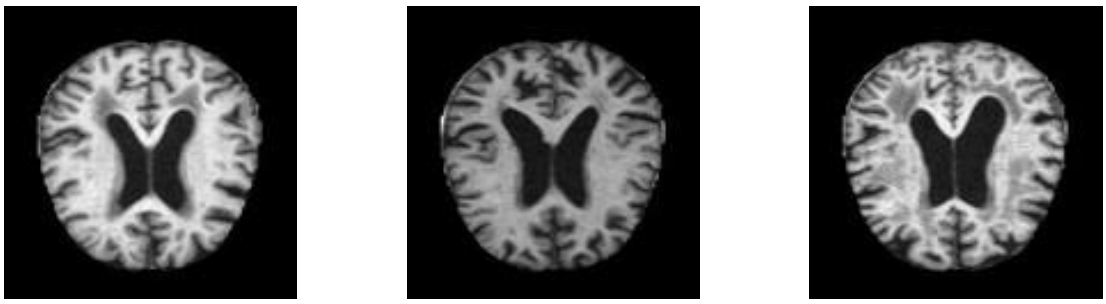

(d) img4 (e) img5 (f) img6

Figure 6: Sample Cover Images of Alzheimer MRI dataset

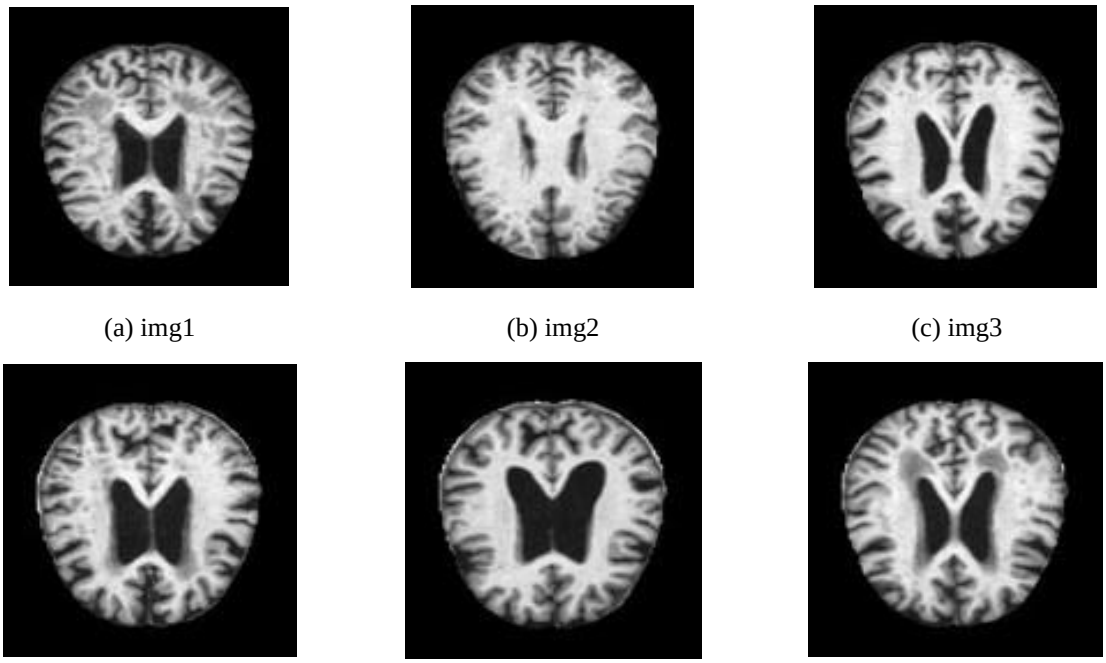

(a) img1 (b) img2 (c) img3

(d) img4 (e) img5 (f) img6

Figure 7: Sample Secret Images of Alzheimer MRI dataset

Figures 8 and 9 show the results of the RIS-CNN Model. It can be observed there is not much difference in both the C_I and encoded C_I as well S_I and decoded S_I.

Doi: https://doi.org/10.54216/FPA.130210
Received: April 17, 2023 Revised: July 19, 2023 Accepted: October 02, 2023

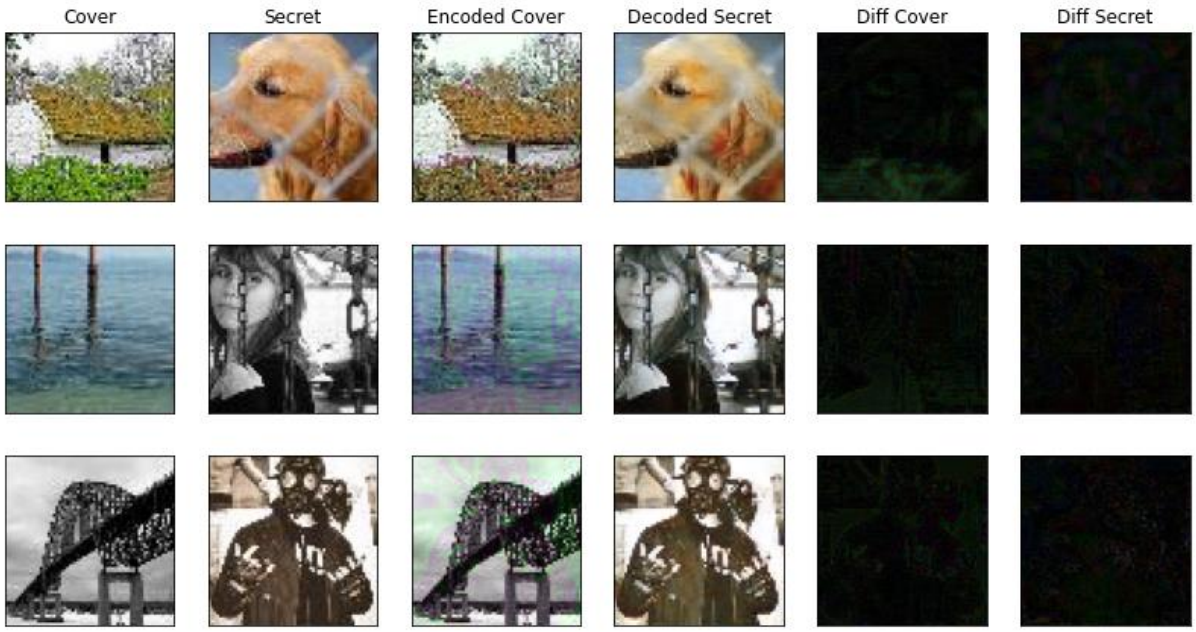

Figure 8: Results of the RIS-CNN Model for TinyImageNet-200 Dataset

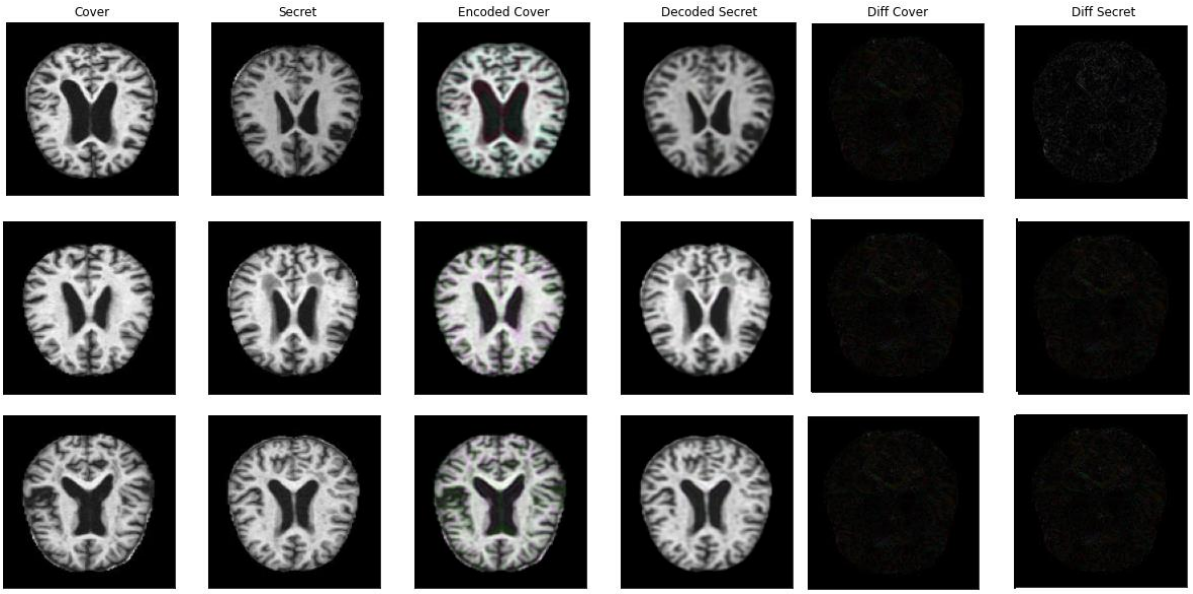

Figure 9: Results of the RIS-CNN Model for Alzheimer's MRI Dataset

Figures 10 and 11 show the results of the RIS – U-Net Model. It can be observed that the difference in both the C_I and encoded C_I as well S_I and decoded S_I is outperforming the previous model.

Doi: https://doi.org/10.54216/FPA.130210
Received: April 17, 2023 Revised: July 19, 2023 Accepted: October 02, 2023

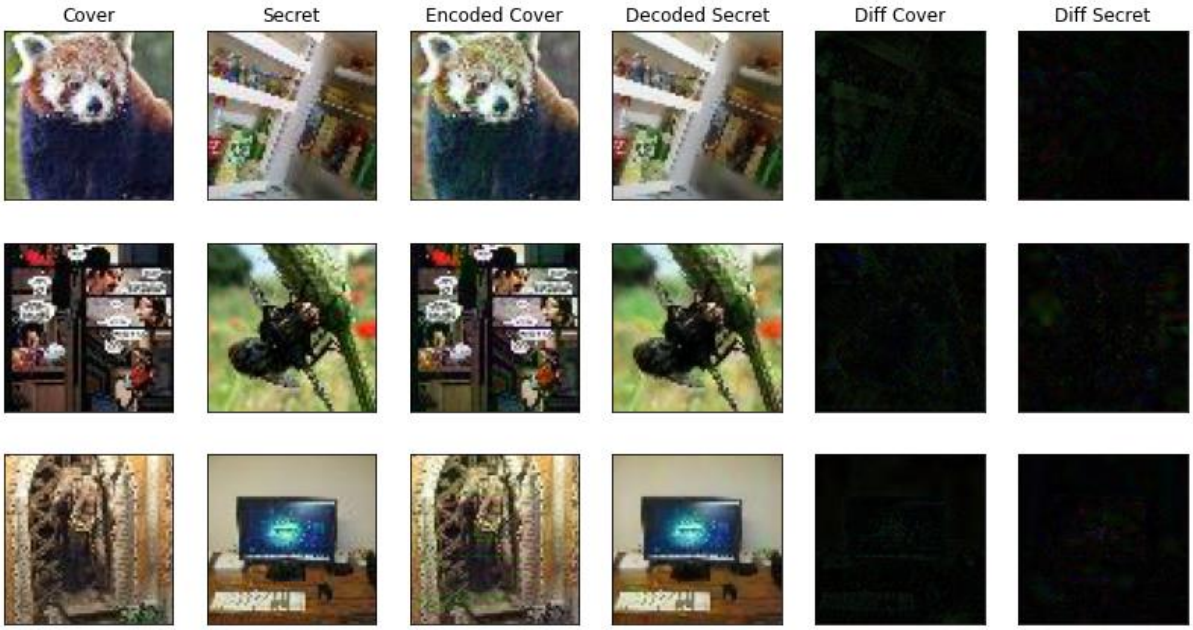

Figure 10: Results of the RIS – U-Net Model for TinyImageNet-200 Dataset

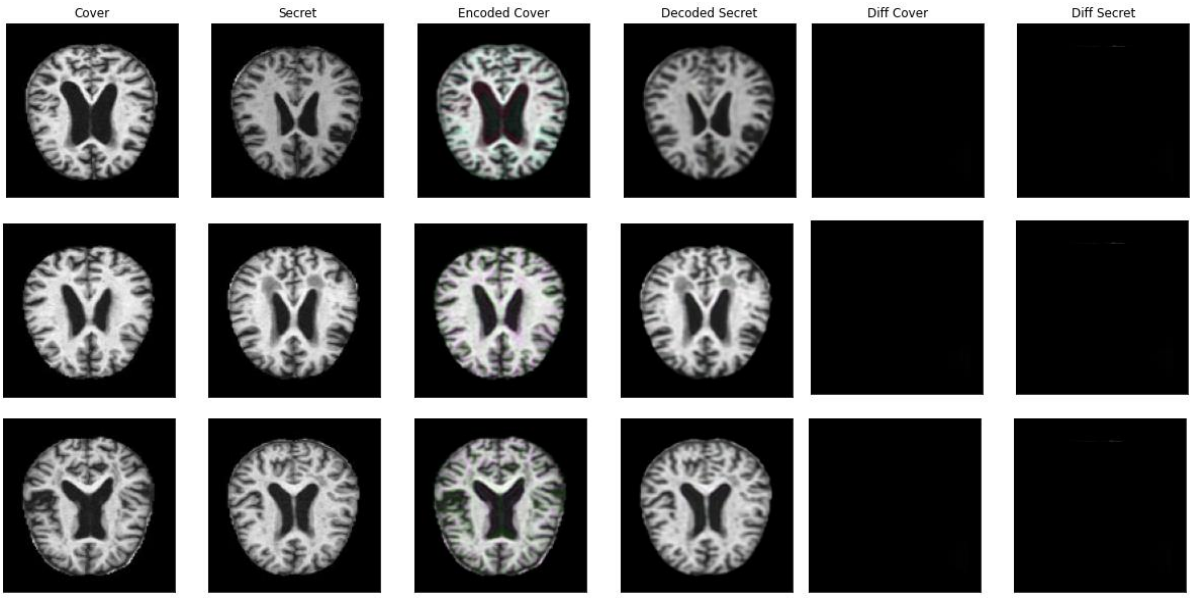

Figure 11: Results of the RIS – U-Net Model for Alzheimer's MRI Dataset

Figures 12 and 13 show the results of the RIS – Circle U-Net Model. It can be observed that the difference in both the C_I and encoded C_I as well secret and decoded S_I is outperforming the previous two models.

Doi: https://doi.org/10.54216/FPA.130210
Received: April 17, 2023 Revised: July 19, 2023 Accepted: October 02, 2023

Figure 12: Results of the RIS – Circle U-Net Model for TinyImageNet-200 Dataset

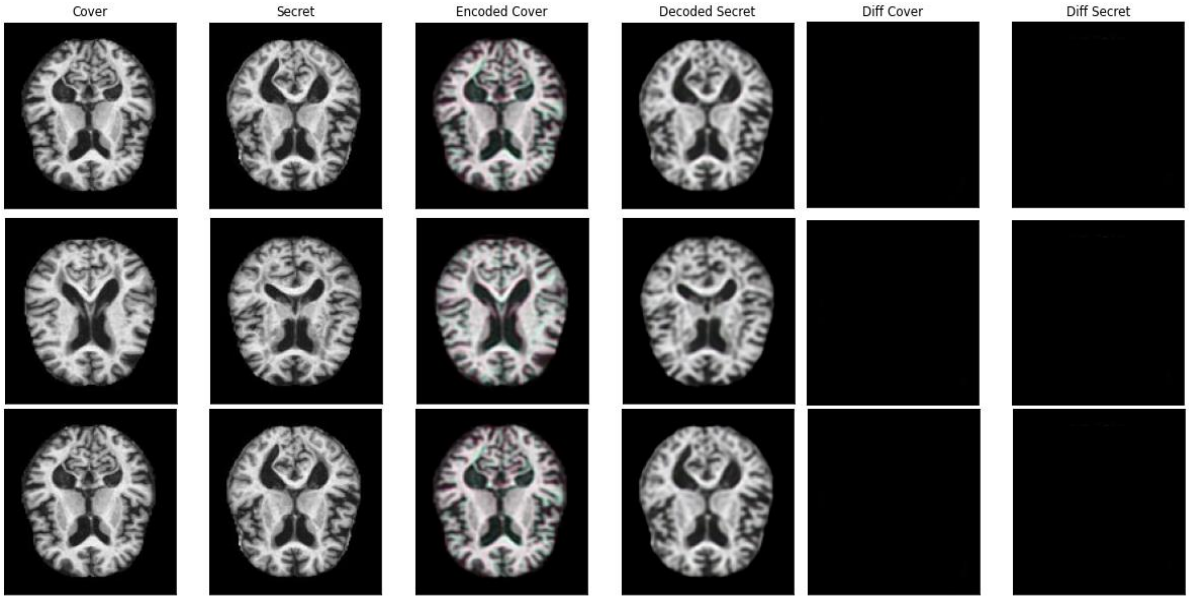

Figure 13: Results of the RIS – Circle U-Net Model for Alzheimer's MRI Dataset

Table 1 shows the performance comparison for different test images of the proposed work with existing works for the TinyImageNet-200 and Alzheimer's MRI Dataset. It is observed that the proposed model outperforms the other two models in terms of MSE, RMSE, PNSR, and SSIM value. A higher PSNR is indicative of superior quality. A SSIM metric approaching a value of 1 signifies a condition of utmost resemblance. The efficiency of the method is substantiated by the notable improvement in both the PSNR and SSIM values.

Table 1: Performance Comparison of Proposed Work with Existing Works

Dataset	Test Image	Performance Metrics	RIS – CNN	RIS – U-Net	RIS – Circle U-Net
TinyImage Net-200	img1	MSE	4.1616	5.7168	2.6211
		RMSE	2.04	2.391	1.619

Doi: https://doi.org/10.54216/FPA.130210
Received: April 17, 2023 Revised: July 19, 2023 Accepted: October 02, 2023

		PSNR	41.93	40.55	43.94
		SSIM	0.9882	0.9822	0.9891
	img2	MSE	5.2212	7.0649	2.7855
		RMSE	2.285	2.658	1.669
		PSNR	40.95	39.63	43.68
		SSIM	0.9726	0.9722	0.9828
	img3	MSE	5.1870	7.2414	2.9377
		RMSE	2.2775	2.691	1.714
		PSNR	40.98	39.53	43.45
		SSIM	0.9759	0.9812	0.9828
Alzheimer's MRI Dataset	img1	MSE	5.8612	4.5326	3.1506
		RMSE	2.421	2.129	1.775
		PSNR	40.45	41.56	43.14
		SSIM	0.9789	0.9873	0.9951
	img2	MSE	4.4605	4.3472	2.7589
		RMSE	2.112	2.085	1.661
		PSNR	41.63	41.74	43.72
		SSIM	0.9896	0.9887	0.9991
	img3	MSE	5.2257	5.9487	2.9618
		RMSE	2.286	2.439	1.721
		PSNR	40.94	40.38	43.41
		SSIM	0.9769	0.9791	0.9858

From the above tables, it can be observed that the RIS– Circle U-Net obtains better PSNR and SSIM values when compared to the rest of the two models. The higher PSNR value indicates that the S_G is less degraded leading to the robustness of the model. On the other end, SSIM values indicate that there is less distortion of the images.

5. Conclusion

The reversible image steganography is carried with the neural network models such as CNN, U-Net scheme, and Circle U-Net structure on TinyImageNet-200 and Alzheimer's MRI dataset. The proposed technique is compared with the RIS using CNN and RIS using U-Net. A Circle-U-Net-based reversible image steganography for effective hiding of image into an image is proposed in this article. It has 101 layers which are motivated by the

Doi: https://doi.org/10.54216/FPA.130210
Received: April 17, 2023 Revised: July 19, 2023 Accepted: October 02, 2023

residual net and circle concepts from geometry. As the layers are deep and residual, the images are hidden better than in other networks. The contracting phase takes care of the concealment of the image. The expanding phase looks upon the reconstruction of the image. The proposed RIS using the Circle-U-Net structure provides better steganographic hiding and extraction capability.

References

[1] Chan, Chi-Kwong, and Lee-Ming Cheng. "Hiding data in images by simple LSB substitution." Pattern recognition 37.3 (2004): 469-474.

[2] Wu, Da-Chun, and Wen-Hsiang Tsai. "A steganographic method for images by pixel-value differencing." Pattern recognition letters 24.9-10 (2003): 1613-1626.

[3] Wu, H-C., et al. "Image steganographic scheme based on pixel-value differencing and LSB replacement methods." IEE Proceedings-Vision, Image and Signal Processing 152.5 (2005): 611-615.

[4] Ni, Zhicheng, et al. "Reversible data hiding." IEEE Transactions on circuits and systems for video technology 16.3 (2006): 354-362.

[5] Barton, James M. "Method and apparatus for embedding authentication information within digital data." United States Patent, 5 646 997 (1997).

[6] Tian, Jun. "Reversible data embedding using a difference expansion." IEEE transactions on circuits and systems for video technology 13.8 (2003): 890-896.

[7] Alattar, Adnan M. "Reversible watermark using the difference expansion of a generalized integer transform." IEEE transactions on image processing 13.8 (2004): 1147-1156.

[8] Kim, Hyoung Joong, et al. "A novel difference expansion transform for reversible data embedding." IEEE Transactions on Information Forensics and Security 3.3 (2008): 456-465.

[9] Lu, Tzu-Chuen, Chun-Ya Tseng, and Jhih-Huei Wu. "Dual imaging-based reversible hiding technique using LSB matching." Signal Processing 108 (2015): 77-89.

[10] Jung, Ki-Hyun. "Dual image based reversible data hiding method using neighbouring pixel value differencing." The Imaging Science Journal 63.7 (2015): 398-407.

[11] Carpentieri, Bruno, et al. "One-pass lossless data hiding and compression of remote sensing data." Future generation computer systems 90 (2019): 222-239.

[12] Nguyen, Thai-Son, Chin-Chen Chang, and Tso-Hsien Shih. "Effective reversible image steganography based on rhombus prediction and local complexity." Multimedia Tools and Applications 77.20 (2018): 26449-26467.

[13] Rahim, Rafia, and Shahroz Nadeem. "End-to-end trained CNN encoder-decoder networks for image steganography." Proceedings of the European Conference on Computer Vision (ECCV) Workshops. 2018.

[14] Baluja, Shumeet. "Hiding images within images." IEEE transactions on pattern analysis and machine intelligence 42.7 (2019): 1685-1697.

[15] Duan, Xintao, et al. "SteganoCNN: image steganography with generalization ability based on convolutional neural network." Entropy 22.10 (2020): 1140.

[16] Zhang, Ru, Shiqi Dong, and Jianyi Liu. "Invisible steganography via generative adversarial networks." Multimedia tools and applications 78.7 (2019): 8559-8575.

[17] Wu, Pin, Yang Yang, and Xiaoqiang Li. "Stegnet: Mega image steganography capacity with deep convolutional network." Future Internet 10.6 (2018): 54.

[18] Hayes, Jamie, and George Danezis. "Generating steganographic images via adversarial training." Advances in neural information processing systems 30 (2017).

[19] Baluja, Shumeet. "Hiding images in plain sight: Deep steganography." Advances in neural information processing systems 30 (2017).

[20] Van, Toan Pham, Thoi Hoang Dinh, and Ta Minh Thanh. "Simultaneous convolutional neural network for highly efficient image steganography." 2019 19th International Symposium on Communications and Information Technologies (ISCIT). IEEE, 2019.

[21] Liu, Lianshan, et al. "A Larger Capacity Data Hiding Scheme Based on DNN." Wireless Communications and Mobile Computing 2022 (2022).

[22] Li, Qi, et al. "A novel grayscale image steganography scheme based on chaos encryption and generative adversarial networks." IEEE Access 8 (2020): 168166-168176.

[23] Chang, Ching-Chun. "Neural reversible steganography with long short-term memory." Security and Communication Networks 2021 (2021).

[24] Tang, Weixuan, et al. "An automatic cost learning framework for image steganography using deep reinforcement learning." IEEE Transactions on Information Forensics and Security 16 (2020): 952-967.

[25] K.P. Ravi Kumar et al.,"Neural Network based Steganography for Information Hiding", International Journal of Recent Technology and Engineering, vol. 8(1S4), 2019.

Doi: https://doi.org/10.54216/FPA.130210
Received: April 17, 2023 Revised: July 19, 2023 Accepted: October 02, 2023

[26] Duan, Xintao, et al. "Reversible image steganography scheme based on a U-Net structure." IEEE Access 7 (2019): 9314-9323.
[27] Sun, Feng, et al. "Circle-u-net: an efficient architecture for semantic segmentation." Algorithms 14.6 (2021): 159.
[28] https://www.kaggle.com/c/tiny-imagenet.
[29] https://www.kaggle.com/datasets/sachinkumar413/alzheimer-mri-dataset.
[30] S. Hemamalini ,V. D. Ambeth Kumar ,R. Venkatesan,S. Malathi.,"Relevance Mapping based CNN model with OSR-FCA Technique for Multi-label DR Classification", Fusion: Practice and Applications, Vol. 11, No. 2, 2023 ,PP. 90-110
[31] C. S. Manigandaa,V. D. Ambeth Kumar,G. Ragunath,R. Venkatesan,N. Senthil Kumar., "De-Noising and Segmentation of Medical Images using Neutrophilic Sets." Fusion: Practice and Applications, Vol.11, No. 2, 2023 ,PP. 111-123.
[32] Qusay Abboodi Ali,Noor M. Sahab. "Interactive Design of a Virtual Classroom Simulation Model Based on Multimedia Applications to Improve the Teaching and Learning Process in the Tikrit University Environment", Fusion: Practice and Applications, Vol. 12, No. 2, 2023 ,PP. 206-216
[33] V. Sathya Preiya,V. D. Ambeth Kumar,R. Vijay,Vijay K.,N. Kirubakaran. "Blockchain-Based E-Voting System with Face Recognition", Fusion Practice and Applications, Vol. 12, No. 1, 2023 ,PP. 53-63
[34] Hamza M. Ridha Al-Khafaji ,Refed Adnan Jaleel. "Design of High-Performance Intelligent WSN based-IoT using Time Synchronized Channel Hopping and Spatial Correlation Model", Fusion: Practice and Applications, Vol. 13, No. 1, 2023 ,PP. 49-58
[35] Balakrishnan, C.; Ambeth Kumar, V.D. IoT-Enabled Classification of Echocardiogram Images for Cardiovascular Disease Risk Prediction with Pre-Trained Recurrent Convolutional Neural Networks. Diagnostics 2023, 13, 775. https://doi.org/10.3390/diagnostics13040775
[36] Sathya Preiya, V.; Kumar, V.D.A. Deep Learning-Based Classification and Feature Extraction for Predicting Pathogenesis of Foot Ulcers in Patients with Diabetes. Diagnostics 2023, 13, 1983. https://doi.org/10.3390/diagnostics13121983

Doi: https://doi.org/10.54216/FPA.130210
Received: April 17, 2023 Revised: July 19, 2023 Accepted: October 02, 2023